

Supporting information for
Anti-freezing hydrogels constructed by pseudo-slide-ring networks

Qianming Lin¹ and Chenfeng Ke^{*1}

¹ Department of Chemistry, Dartmouth College, 41 College Street, Hanover, New Hampshire,
US

Contact: chenfeng.ke@dartmouth.edu

S1. General information

All reagents were purchased from commercial suppliers and used as received, unless otherwise specified. The α -Cyclodextrin (α -CD) was generously gifted by Wacker Chemical Corporation.

Nuclear magnetic resonance (NMR) spectra were recorded on Bruker Advance 500 MHz spectrometers with working frequencies of 500 MHz for ^1H . Chemical shifts are reported in ppm relative to the residual non-deuterated solvent signals (CDCl_3 : $\delta = 7.26$ ppm, $\text{DMSO}-d_6$: $\delta = 2.50$ ppm, D_2O : $\delta = 4.79$ ppm). Fourier transform infrared (FT-IR) spectra were collected on a Shimadzu IRAffinity-1 FTIR-8000 spectrometer. Uniaxial tensile tests were performed on a stress-controlled rheometer (TA instruments, DHR-2). The strain rate was $20 \mu\text{m/s}$. Differential scanning calorimeters (DSC) measurements were performed on a Discovery DSC 250 (TA instruments). Scanning started at 10°C and went to -50°C at a rate of 5°C per min. Resistances were measured by a universal meter. Optical images were recorded on a consumer-grade camera.

S2. Synthetic methods

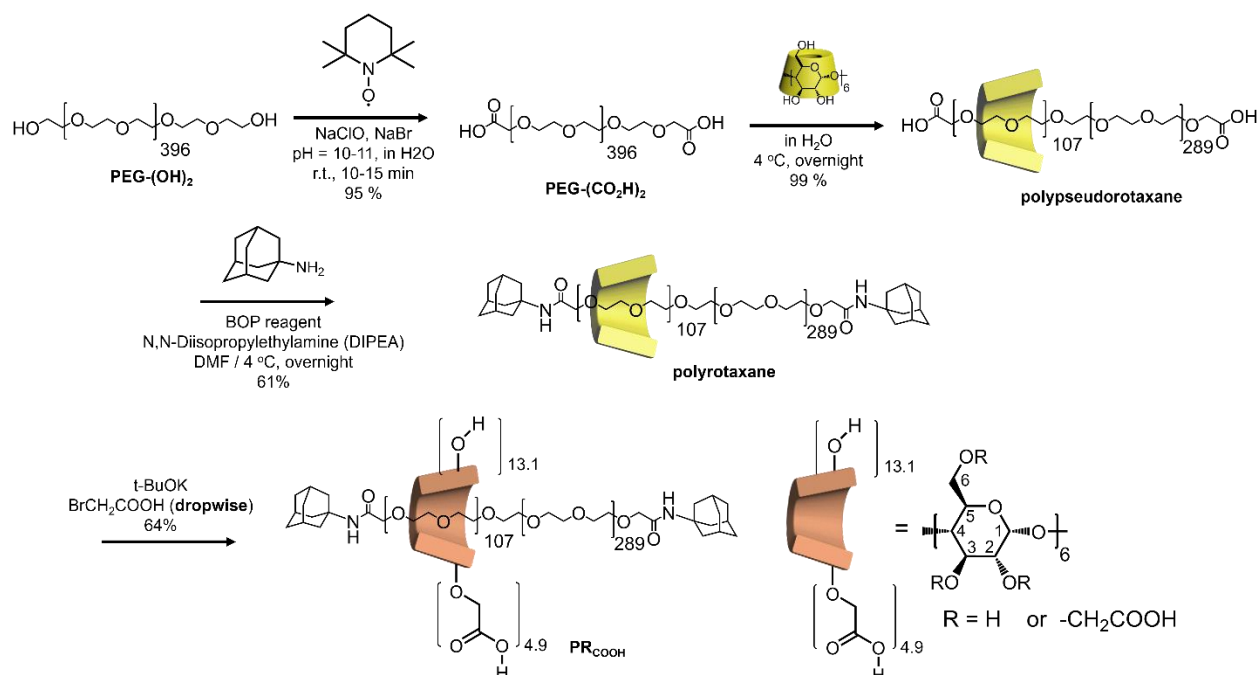


Figure S1. Synthetic scheme of the polyrotaxane crosslinker PR_{COOH}

The polyrotaxane crosslinker PR_{COOH} was synthesized following a previously reported method.¹

Synthesis of PEG_{35k}-(CO₂H)₂. PEG-(CO₂H)₂ was synthesized by oxidation of the terminal hydroxyl groups of PEG-(OH)₂ (Mn = 35kDa) using 2,2,6,6-tetramethyl-1-piperidinyloxy radical (TEMPO). PEG_{35k}-OH (30.0 g, 0.86 mmol) was dissolved in water (300 mL). TEMPO (300 mg, 1.92 mmol), NaBr (3.0 g, 30 mmol), and aqueous NaClO (15 mL, available chlorine > 5.0%) at pH 10-11 were added to the reaction at room temperature and stirred for 15 min. The reaction was quenched by the addition of 10 mL of ethanol, followed by acidification using aqueous HCl to reduce the reaction pH to < 2. The product was extracted three times using dichloromethane (3 × 100 mL). The product was collected by precipitation in diethyl

ether, followed by a re-precipitation to afford the desired PEG-(COOH)₂ as a white solid (yield: 95 %). ¹H NMR (500 MHz, CDCl₃): δ (ppm) = 4.21 (-CH₂COOH), 3.8-3.3 (-CH₂- of PEG).

Synthesis of the native α-CD-based polyrotaxane. The Ad-polyrotaxane was prepared using 1-adamantanamine as the stopper. PEG_{35k}-CO₂H (12.0 g, 0.34 mmol) and α-CD (48.0 g, 49.4 mmol) were dissolved in water (360 mL) and kept in a refrigerator (4 °C) overnight, affording a white, paste-like polypseudorotaxane intermediate. The polypseudorotaxane intermediate was lyophilized. The freeze-dried polypseudorotaxane intermediate (15.0 g, 0.09 mmol), 1-adamantanamine (1.3 g, 8.6 mmol), (benzotriazol-1-yloxy)tris(dimethylamino)-phosphonium hexafluoro-phosphate (BOP, 0.38 g, 0.86 mmol), and *N,N*-diisopropylethylamine (DIPEA, 0.15 mL, 0.86 mmol) were mixed in anhydrous dimethylformamide (DMF, 50 mL) to form a slurry, which was stirred at 4 °C overnight to allow for a heterogeneous reaction. The product was washed two times with DMF/methanol (1:1) and two times with methanol. The crude product was dissolved in DMSO (80 mL), and the solution was poured into water (800 mL) to form a precipitate, which was then collected by centrifugation. The product was further washed with an excess of water followed by two more centrifugations. The obtained off-white solid was lyophilized to afford the Ad-polyrotaxane as a white solid (yield: 61 %). ¹H NMR (500 MHz, DMSO-d₆): δ (ppm) = 6.79 (-NH-CO-), 5.64 (OH-2 of α-CD), 5.49 (OH-3 of α-CD), 4.79 (H-1 of α-CD), 4.42 (OH-6 of α-CD), 3.9-3.4 (H-3, H-5, H-6 of α-CD and -CH₂- of PEG_{35k}), 3.4-3.2 (H-2 and H-4 from α-CD of α-CD), 2.0 (-CH₂- of Ad), 1.9 (-CH- of Ad), 1.6 (-CH₂- of Ad). The average number of α-CD threaded on each PEG axle was calculated to be 107 using ¹H NMR analysis, corresponding to a threading ratio of ca. 27%.

Synthesis of partially carboxymethylated polyrotaxane PR_{COOH}. The obtained polyrotaxane was partially carboxymethylated using bromoacetic acid and potassium tert-butoxide. Polyrotaxane (0.7 g, 0.004 mmol) and potassium tert-butoxide (5.2 g, 47 mmol) were dissolved in 30 mL anhydrous DMSO, and bromoacetic acid (6.5 g, 47 mmol) dissolved in 30 mL anhydrous DMSO was added dropwise. The mixture was stirred overnight. The crude product was purified by dialysis against deionized water, followed by a freeze-drying process. Then, the obtained powder was rigorously washed with an excess of DCM and ethanol. After washing, the collected solid was dried to afford the partially carboxymethylated polyrotaxane as a slightly yellow powder (yield: 64%). ¹H NMR (500 MHz, D₂O): δ (ppm) = 5.21 (H-1 of α-CD), 4.98 (H-1 of α-CD), 4.4-4.05 (-OCH₂-COOH of α-CD), 4.0-3.4 (H-3, H-5, H-6 of α-CD and -CH₂- of PEG_{35k}), 3.5-3.35 (H-2 and H-4 from α-CD), 2.0 (-CH₂- of Ad), 1.9 (-CH- of Ad), 1.6 (-CH₂- of Ad). The average number of carboxymethyl groups on each α-CD was calculated to be 4.9 ± 0.3 using ¹H NMR analysis, corresponding to a substitution degree of 27 ± 2 %. The average substitution degree and its corresponding statistical error was calculated by analyzing three parallel experimental results.

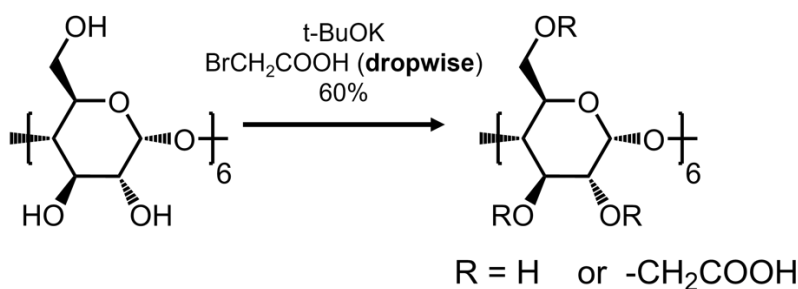


Figure S2. Synthesis of partially carboxymethylated α-CD

Synthesis of partially carboxymethylated CD. α -CD (5 g, 5.1 mmol) and potassium tert-butoxide (7.54 g, 3.4 mmol) were dissolved in 50 mL anhydrous DMSO, and bromoacetic acid (4.3 g, 1.7 mmol) dissolved in 50 mL anhydrous DMSO was added dropwise. The mixture was stirred overnight. The crude product was precipitated by adding an excess of ethanol, and the precipitate was then rigorously washed with an excess of ethanol three times. After washing, the collected solid was dried afford the partially carboxymethylated α -CD as a slightly yellow powder (yield: 60%). $^1\text{H NMR}$ (500 MHz, D_2O): δ (ppm) = 5.21 (H-1 of α -CD), 4.98 (H-1 of α -CD), 4.4-4.05 ($-\text{OCH}_2\text{-COOH}$ of α -CD), 4.0-3.4 (H-3, H-5, H-6 of α -CD), 3.7-3.35 (H-2 and H-4 from α -CD of α -CD). The average number of carboxymethyl groups on each α -CD was calculated to be 4.7 using $^1\text{H NMR}$ analysis, corresponding to a substitution degree of 26 %.

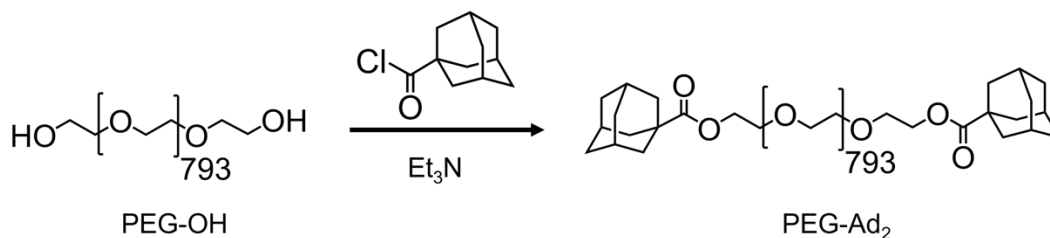


Figure S3. Synthesis of the PEG-Ad₂

Synthesis of PEG-Ad₂. In a 100 mL round bottom flask, anhydrous PEG-OH (Mn = 35kDa, 1g, 0.029 mmol) and triethylamine (Et_3N , 80 μL , 0.58 mmol) were dissolved in anhydrous DCM (30 mL) in an ice-bath. 1-Adamantanecarboxylic acid chloride (114 mg, 0.58 mmol) was added to the reaction dropwise, and the reaction mixture was stirred for another 24 h at 20 °C. After that, the reaction was washed by 1M HCl aqueous solution (50 mL \times 2), saturated NaHCO_3 solutions (50 mL \times 2), brine (50 mL) and dried over Na_2SO_4 . The product was collected by precipitation in ethyl ether, followed by another re-precipitation process to afford a white solid (yield: 80%). $^1\text{H NMR}$ (500 MHz, D_2O): δ (ppm) = 3.63 ($-\text{CH}_2-$ of PEG), 1.99 ($-\text{CH}_2-$ of Ad), 1.87 ($-\text{CH}-$ of Ad), 1.70 ($-\text{CH}_2-$ of Ad).

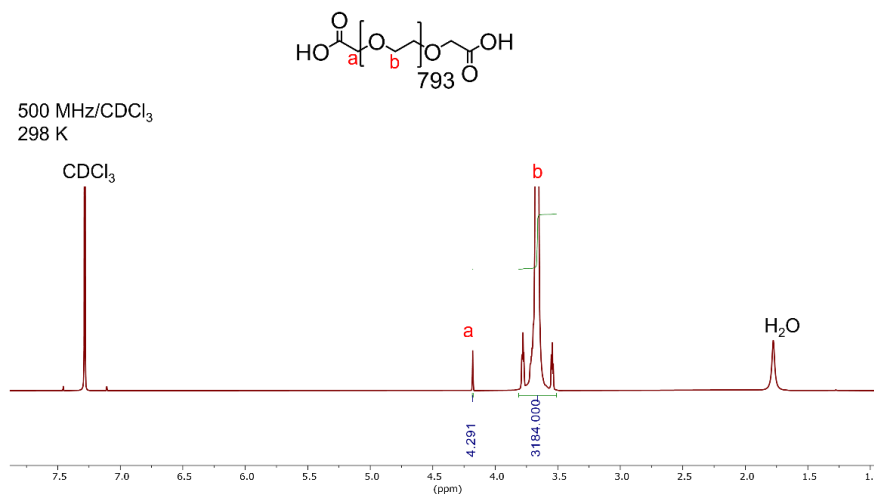
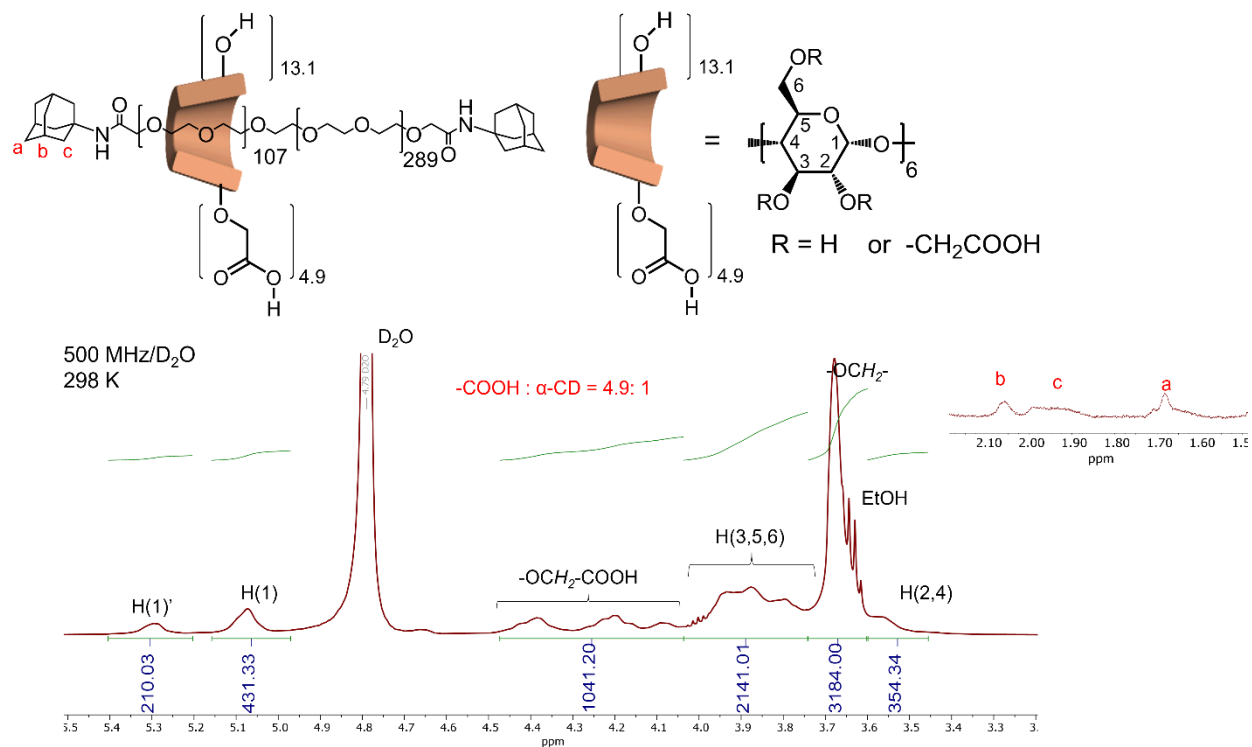
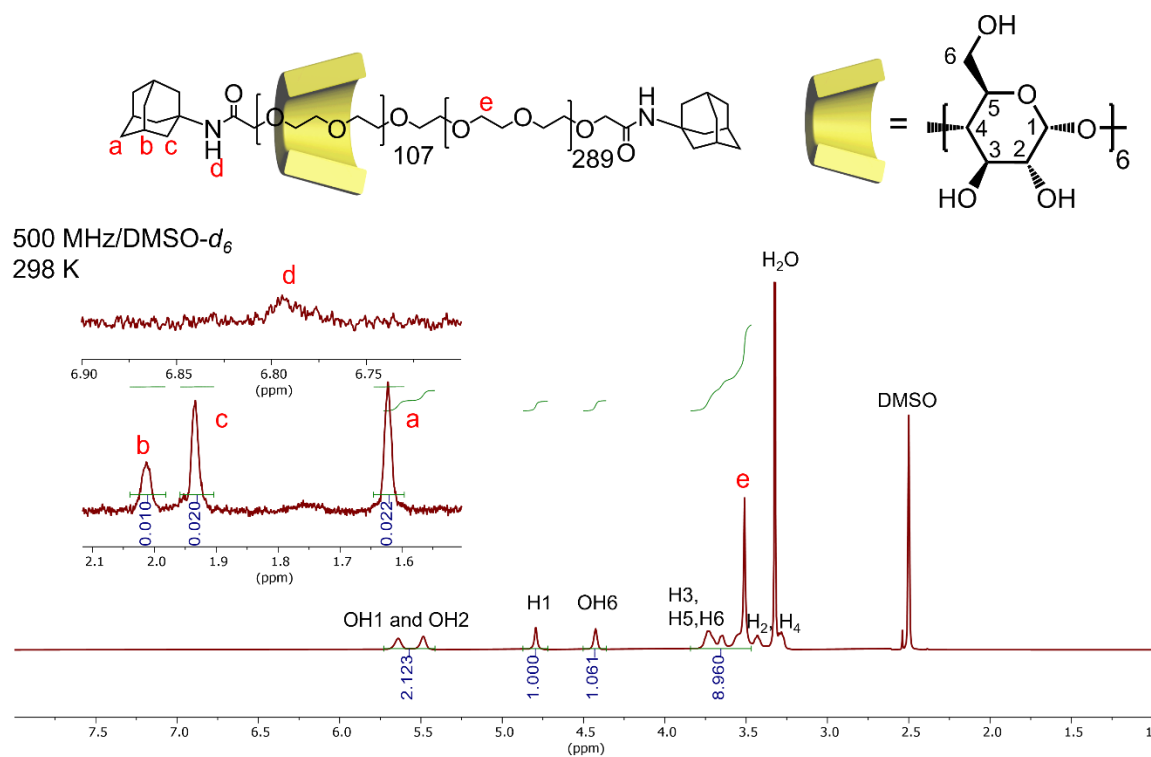


Figure S4. $^1\text{H NMR}$ spectrum of PEG-(COOH)₂. (500 MHz, CDCl_3 , 298 K)



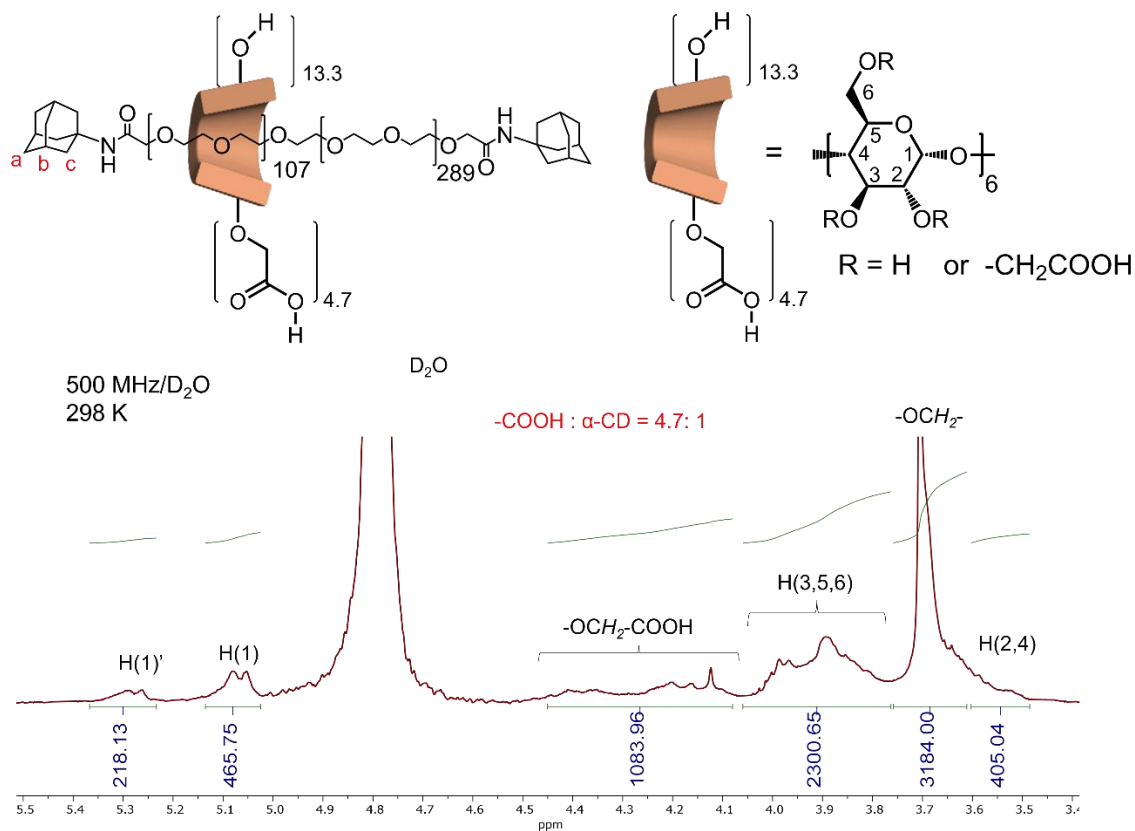


Figure S7. ¹H NMR spectrum of carboxymethylated polyrotaxane (PR_{COOH}, 500 MHz, D₂O, 298 K)

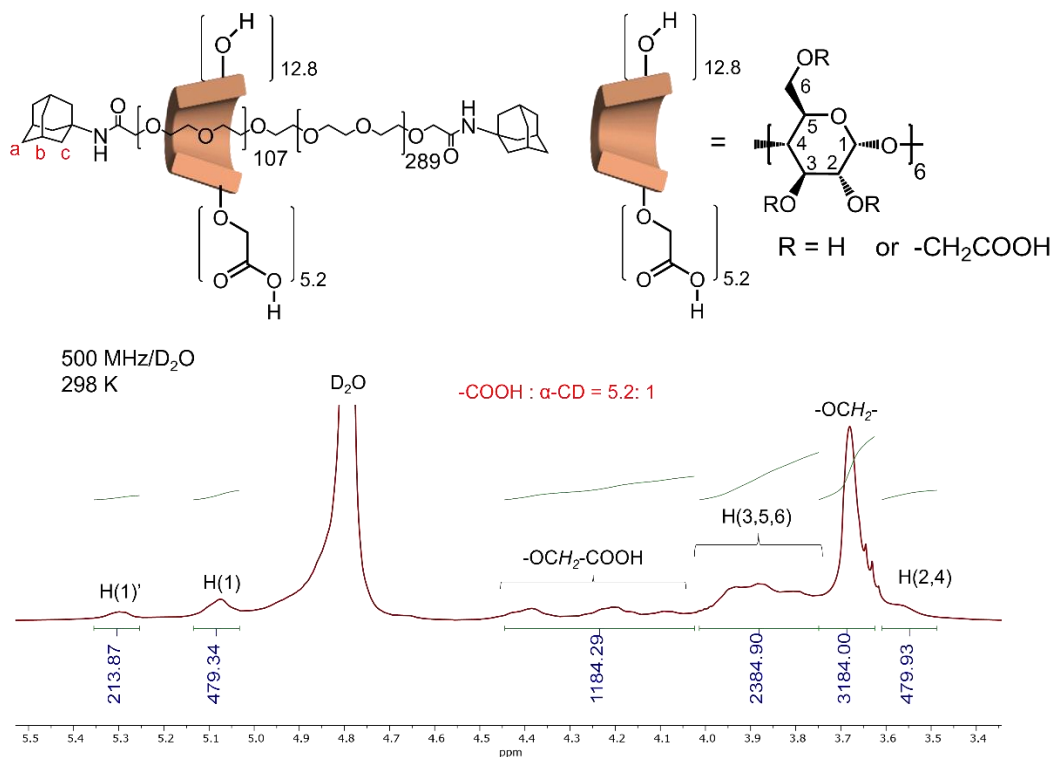


Figure S8. ¹H NMR spectrum of carboxymethylated polyrotaxane (PR_{COOH}, 500 MHz, D₂O, 298 K)

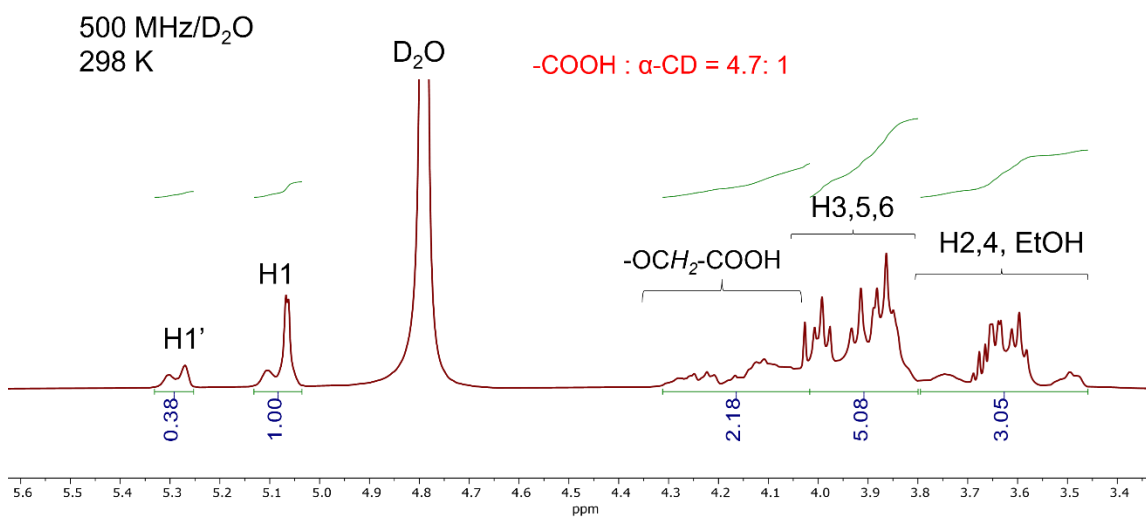
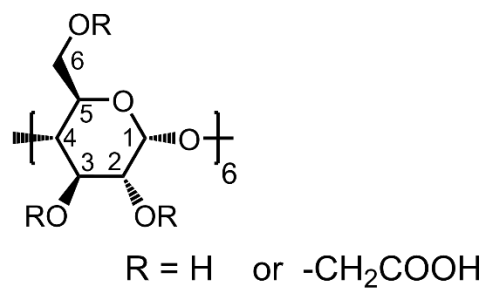


Figure S9. ¹H NMR spectrum of carboxymethylated α -CD (500 MHz, D₂O, 298 K)

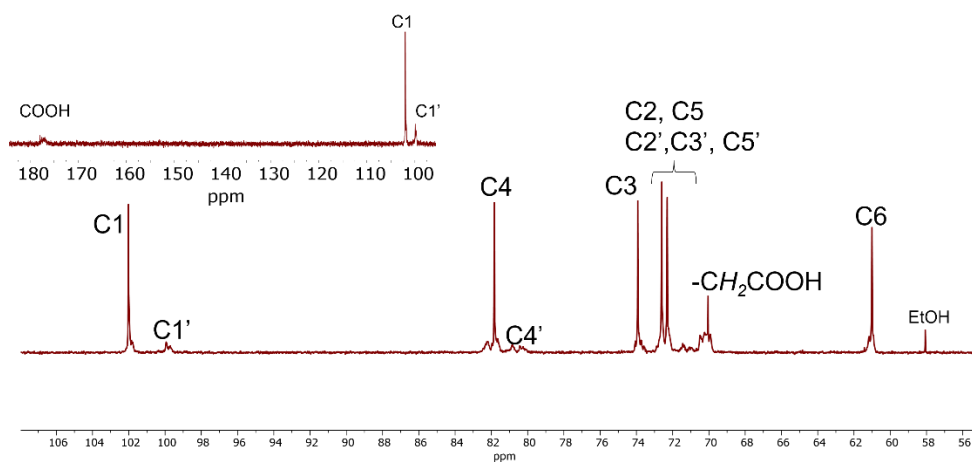
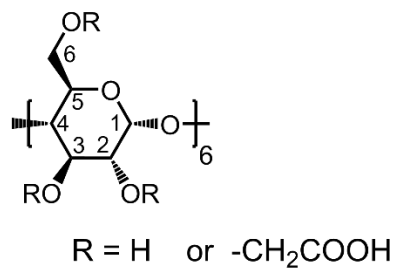


Figure S10. ¹³C NMR spectrum of carboxymethylated α -CD (150 MHz, D₂O, 298 K)

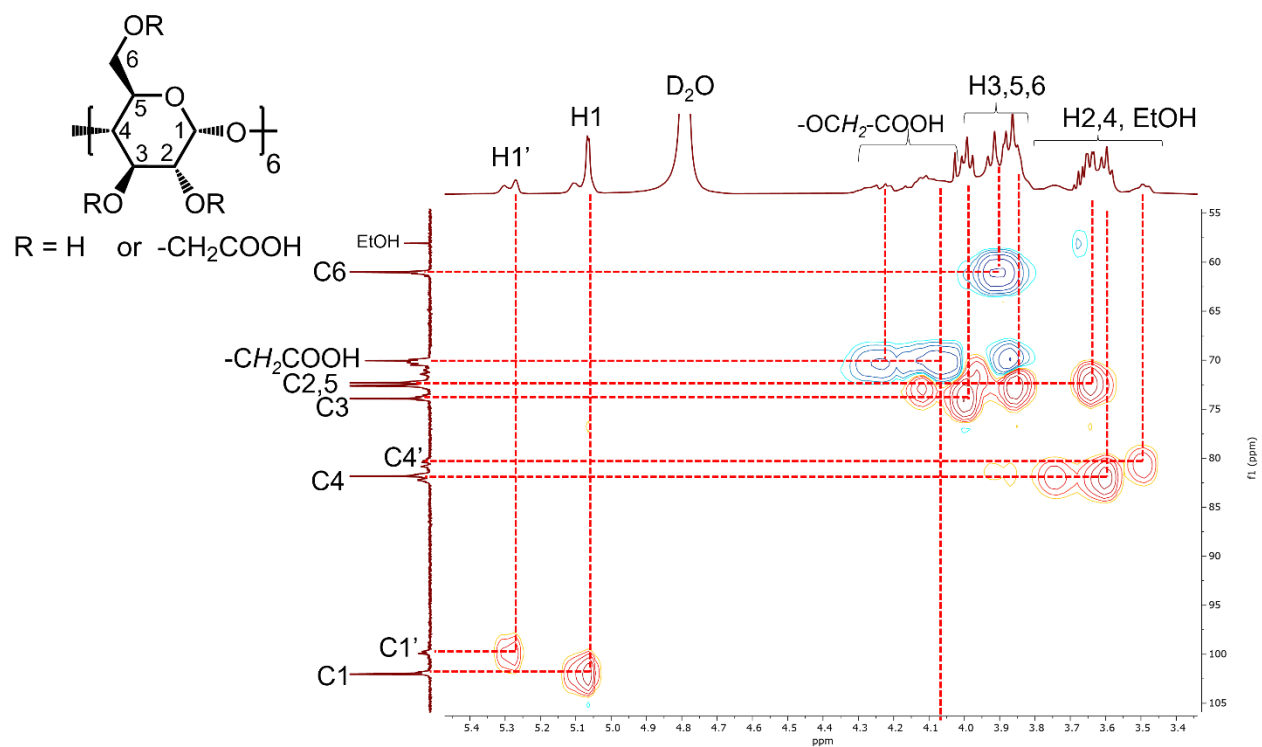


Figure S11. Heteronuclear single quantum coherence (HSQC) NMR spectrum of carboxymethylated α -CD (600 MHz, D_2O , 298 K)

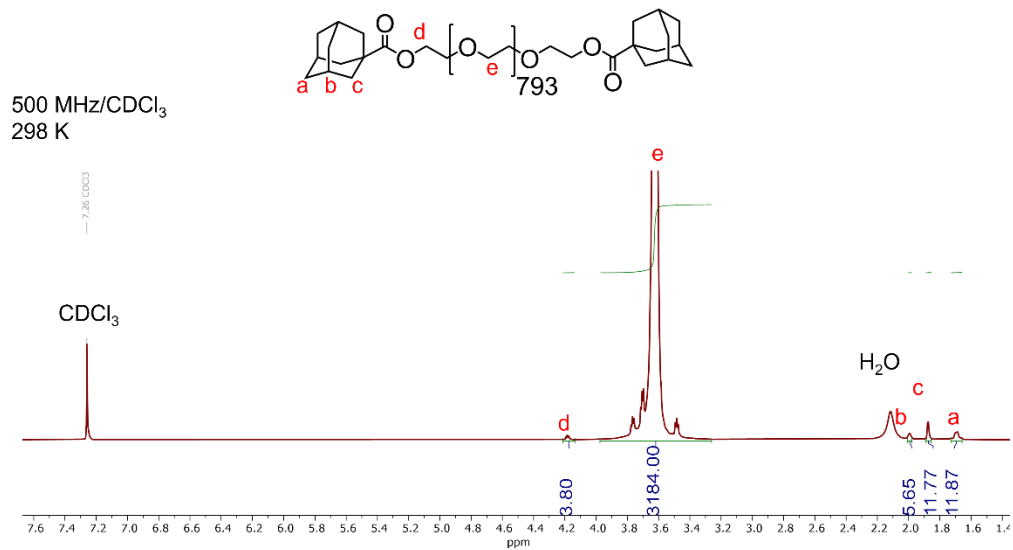


Figure S12. 1H NMR spectrum of PEG-Ad₂ (500 MHz, $CDCl_3$, 298 K)

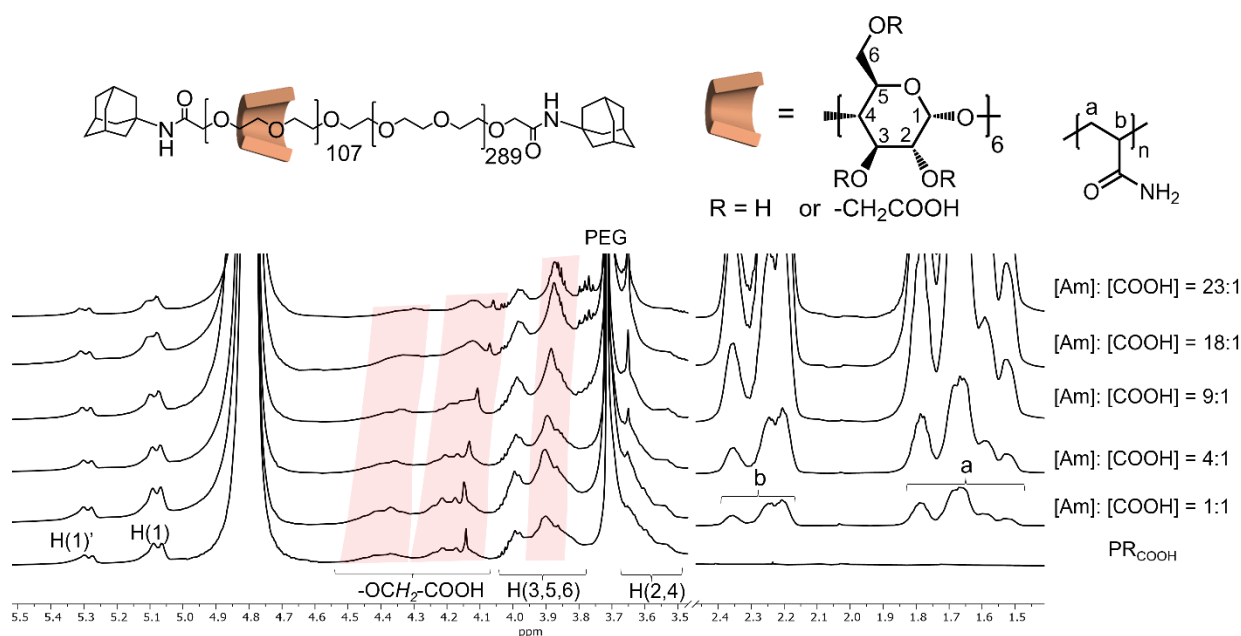


Fig. S13. ^1H NMR spectra (600 MHz, D_2O) of PR_{COOH} ($[\text{COOH}] = 7 \text{ mM}$) titrated with PAAm at $[\text{Am}]$: $[\text{COOH}]$ ratios of 0, 1, 4, 9, 18 and 23, respectively.

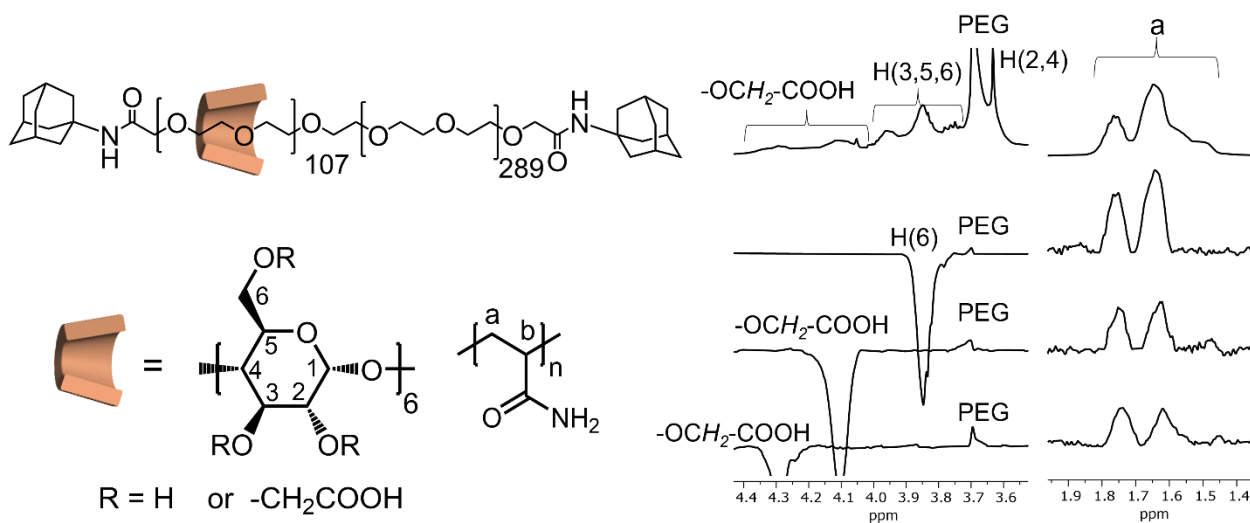


Fig. S14. ^1H NMR (top right) and 1D NOE (bottom right three spectra) spectra of the PR_{COOH} /PAAm complex at a $[\text{Am}]$: $[\text{COOH}]$ ratio of 23 :1. The carboxymethyl resonances of PR_{COOH} at 4.29, 4.10 and H6 proton of α -CD at 3.85 ppm were selectively irradiated.

Preparation of PR_{COOH} solution and hydrogels. Various quantities of PR_{COOH} powder (1-20 wt%) were dissolved in water at 60°C , and then cooled to room temperature to afford solutions of PR_{COOH} or hydrogels. The hydrogels could undergo redissolution upon reheating at 60°C .

Table S1. The summary of the PR_{COOH} samples prepared by dissolving varied amount of PR_{COOH} in water.

[PR _{COOH}] wt%	1	5	10	20
[PR _{COOH}] mM	0.06	0.3	0.6	1.2
[COOH] mM	31	155	310	620
image				
solution(sol) or hydrogel (gel)	sol	sol	sol	gel

Synthesis of PAAm and PSR hydrogels. Acrylamide monomer (0.2 g, 2.8 mmol, 20 wt%) powder, N,N'-methylenebisacrylamide crosslinker (MBAA, fixed at 0.0084 equivalents to 1 equivalent of acrylamide monomer) and PR_{COOH} (2, 5, and 10 wt%, 0.05, 0.13, 0.26 M of carboxylic group, respectively) were dissolved in 1 mL degassed water. The pH of solution was changed to 4 with addition of a concentrated HCl solution. After that, the radical initiator ammonium persulfate (APS, 4 mg, 22 mM) and the catalyst tetramethylethylenediamine (TEMED, 8 ul, 67 mM) were added to the reaction mixture. After mixing, the solution was poured into a TeflonTM mold and crosslinked at 20 °C overnight affording **PAAm**, **PSR_{2wt}**, **PSR_{5wt}**, and **PSR_{10wt}**, where the number denotes the wt% of PR_{COOH}. After crosslinking, the hydrogels were demolded and dried in a sealed chamber with saturated sodium bromide solution to lower the water content to 50 ± 3 %. The control hydrogel CH_{5wt} was synthesized using PEG-Ad₂ and carboxymethylated α-CD (4.7 carboxymethyl groups per α-CD molecule). The CH_{5wt} hydrogel had the same molecular entities as the PSR_{5wt} at identical concentration, but the carboxymethylated CDs were not mechanically interlocked.

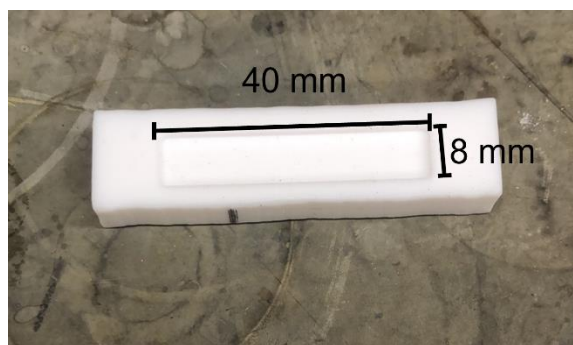


Figure S15. Image of rectangular TeflonTM mold (40 × 8 × 2 mm).

S3. Materials characterization

Rheological measurements. The PAAm/PR_{COOH} samples were prepared by mixing PR_{COOH} (20 wt%, 0.62 M of carboxylic group) and different amounts of linear PAAm ($M_n = 10$ kDa, 0, 2.46, 5.56, 11.13, and 14.08 M of amide group, respectively). The ratio of the amide/carboxylic acid was varied from 0 to 23:1. PAAm solutions at different concentrations were also prepared as comparison. Rheological measurements were performed on a stress-controlled rheometer (TA instruments, DHR-2) with a 20-mm diameter parallel

plate geometry and a measuring gap of 1 mm at room temperature. *Oscillation strain sweep test.* Strain sweep tests were performed to investigate the linear viscoelastic regions of the obtained polypseudorotaxane hydrogels at 25 °C. The oscillation strain was increased from 0.01% to 100%. The angular frequency was set at 1 rad/s. *Angular frequency sweep test.* Angular frequency sweep tests were performed to investigate the elastic and viscous moduli at 25 °C. The angular frequency was increased from 0.1 rad/s to 100 rad/s. The oscillation strain was set at 0.1 %. *Steady rate sweep test.* Steady rate sweep tests were carried out to investigate the flow behaviors. The shear rate was increased from 1 s⁻¹ to 100 s⁻¹.

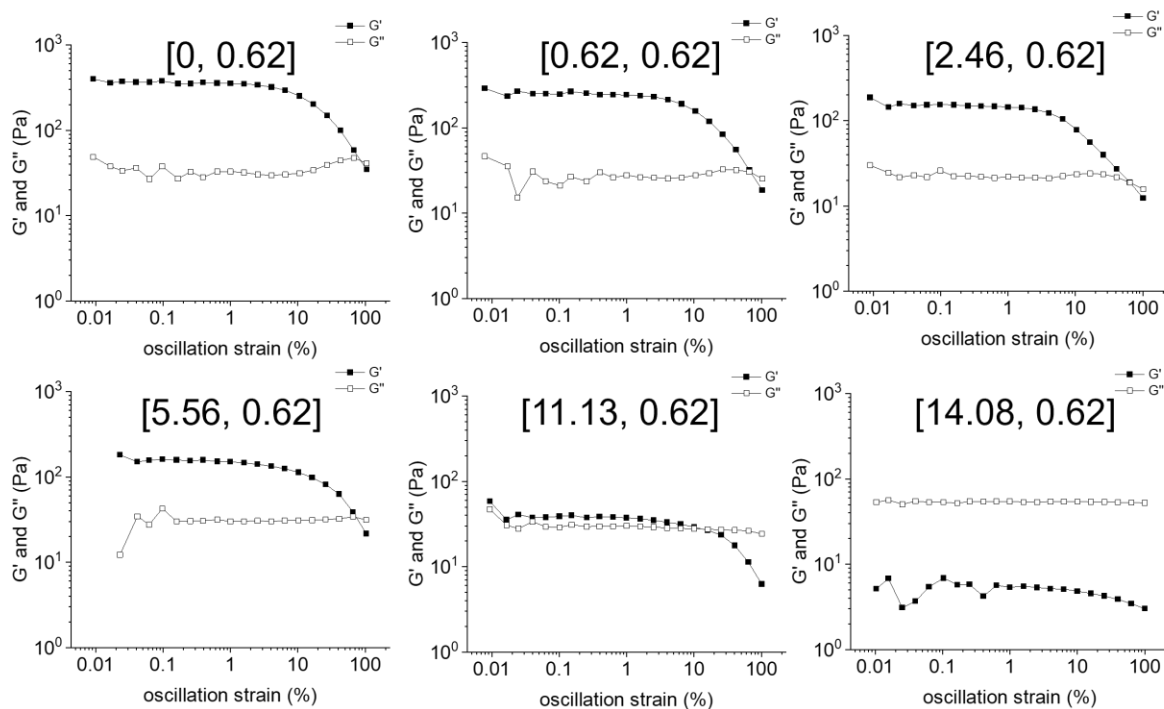


Figure S16. Oscillation strain sweeps of the samples formed by PR_{COOH} (20 wt%, 0.62 M of carboxylic group) and different amounts of linear PAAm (0, 2.46, 5.56, 11.13, 14.08 M of amide group, respectively). The ratio between the amide/carboxylic acid was varied from 0 to 23:1. The numbers within the brackets represent the concentration of amide and carboxylate acid groups in M, accordingly.

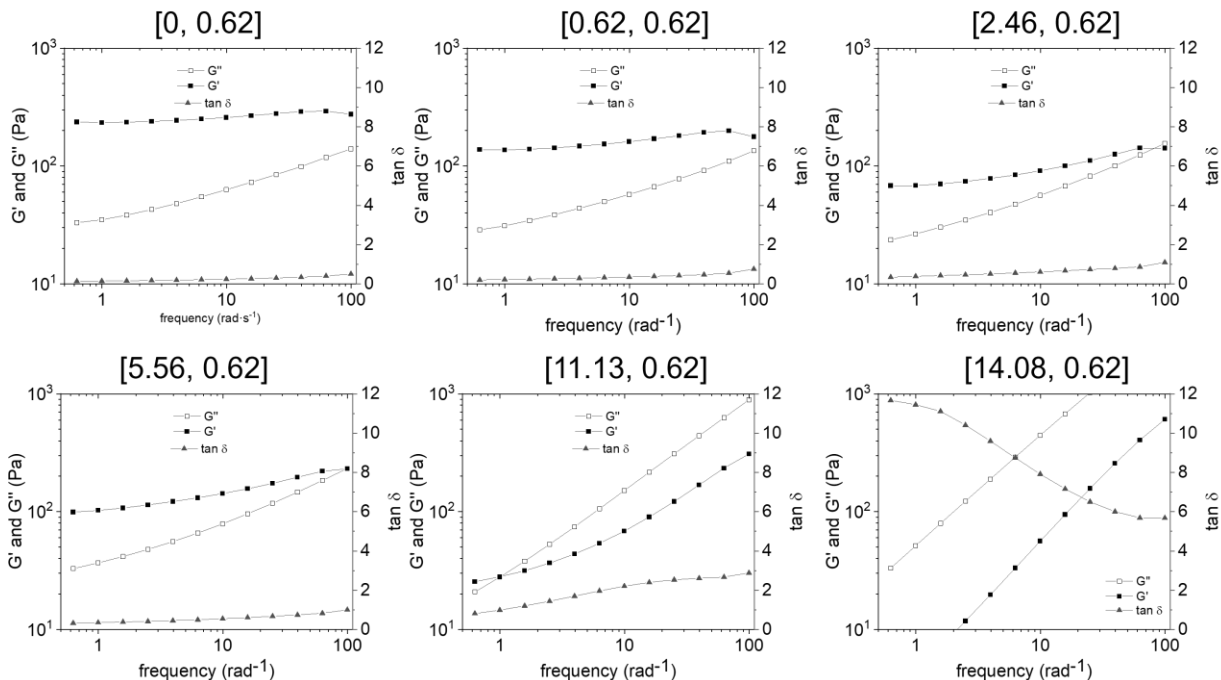


Figure S17. Frequency sweeps of the samples formed by PR_{COOH} (20 wt%, 0.62 M of carboxylic group) and different amounts of linear PAAm (0, 2.46, 5.56, 11.13, 14.08 M of amide group, respectively).

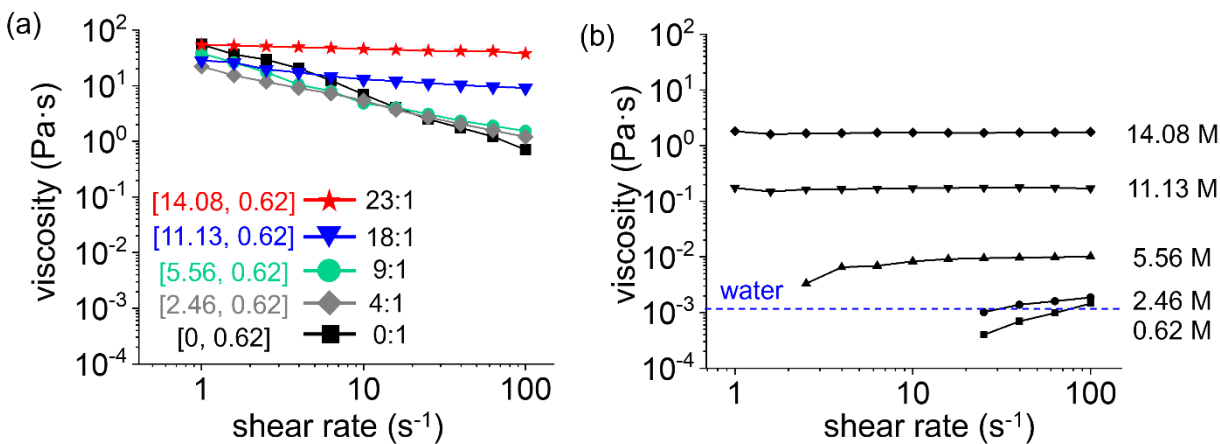


Figure S18. Shear sweeps of (a) the samples formed by PR_{COOH} (20 wt%, 0.62 M of carboxylic group) and different amounts of linear PAAm (0, 2.46, 5.56, 11.13, 14.08 M of amide group, respectively) and (b) PAAm solutions.

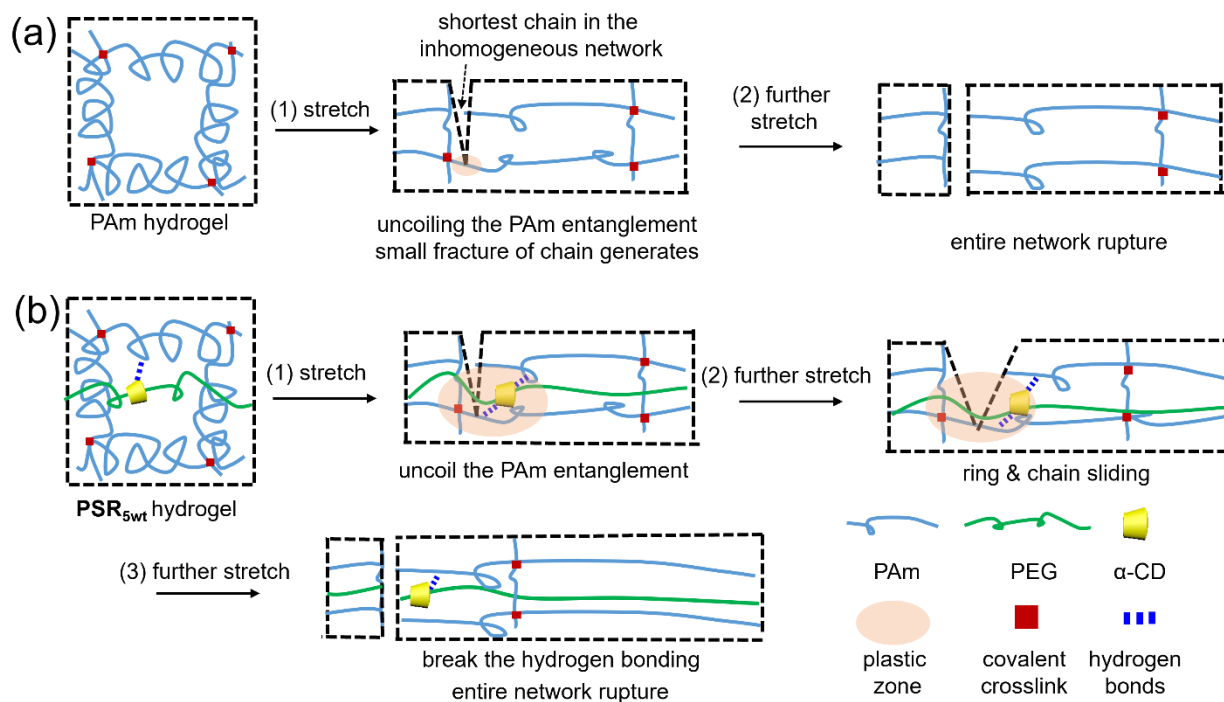


Figure S19. Schematic illustration of proposed mechanism for energy dissipation in the networks of (a) pure **PAAm** and (b) **PSR_{5wt}** hydrogel under stretching.

Our proposed mechanism is that under stretching, the uncoiling of the PAAm chain entanglement will first take place until some of the shortest chains break, due to the inhomogeneity in a conventional covalent crosslinked network. And once the chains break, the energy stored in the entire system will dissipate and the fracturing of chains will proceed under further stretching, finally causing the rupture of the entire network. In the **PSR_{5wt}**, under further stretching, the rings will slide before the breakage of hydrogen bonds. At a higher strain, the hydrogen bonds between carboxymethylated CDs and amide groups of PAAm will first break, and then re-form as the sliding rings shift to the neighboring amide groups so that the chains of PAAm can be further pulled out. When the applied strain is further increased, the hydrogen bonds will break and the propagating cracks of PAAm chains proceed to grow larger, rupturing of the entire network. Hence, both sliding crosslinks and hydrogen bonds contribute to the energy dissipation in **PSR_{5wt}**, while in PAAm, the rupturing results from localized damage, which affords a small fracture energy.

Stress-strain curves measurements at different temperature. Pure **PAAm**, **PSR_{2wt}**, **PSR_{5wt}**, **PSR_{10wt}** and **CH_{5wt}** hydrogels were prepared by molding the precursor solutions into rectangular specimens. After crosslinking, the hydrogels were dried in a sealed chamber until the water content was decreased to $50 \pm 3\%$. The Young's modulus, the strain at break, and toughness were measured by uniaxial tensile tests with a strain rate of $20 \mu\text{m/s}$ until rupture. The mechanical tests were performed at 20°C , -14°C , and -22°C .

Cyclic loading and unloading tests at 20°C . Uniaxial tensile loads were applied to pure **PAAm**, **CH_{5wt}**, and **PSR_{5wt}** with a strain rate of $20 \mu\text{m/s}$. After the applied strain reached 50% or 100%, the stress was unloaded. The second load was applied immediately after the unloading in the former cycle finished. The cycle of loading and unloading was repeated three times.

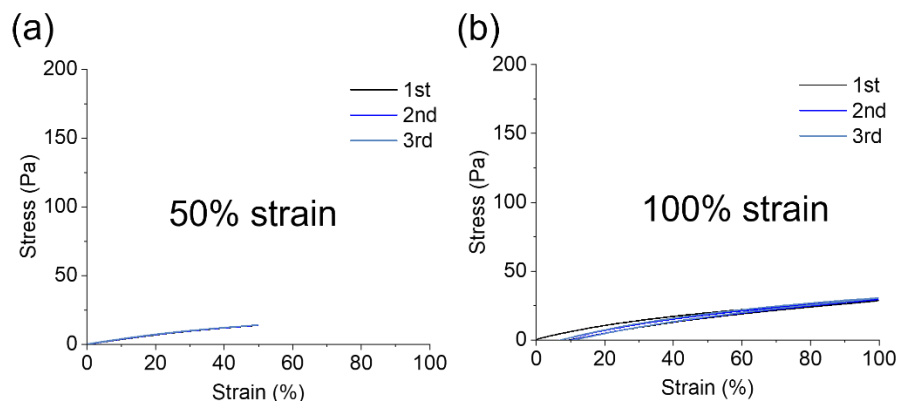


Figure S20. Cyclic loading and unloading of uniaxial stress tests of pure **PAAm** with a strain rate of 20 $\mu\text{m/s}$ until (a) 50% and (b) 100% strain at 20 $^{\circ}\text{C}$.

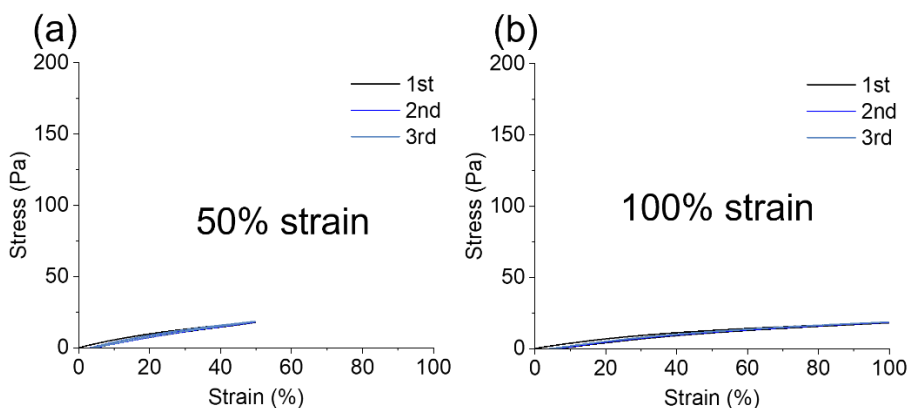


Figure S21. Cyclic loading and unloading of uniaxial stress tests of **CH_{5wt}** with a strain rate of 20 $\mu\text{m/s}$ until (a) 50% and (b) 100% strain at 20 $^{\circ}\text{C}$.

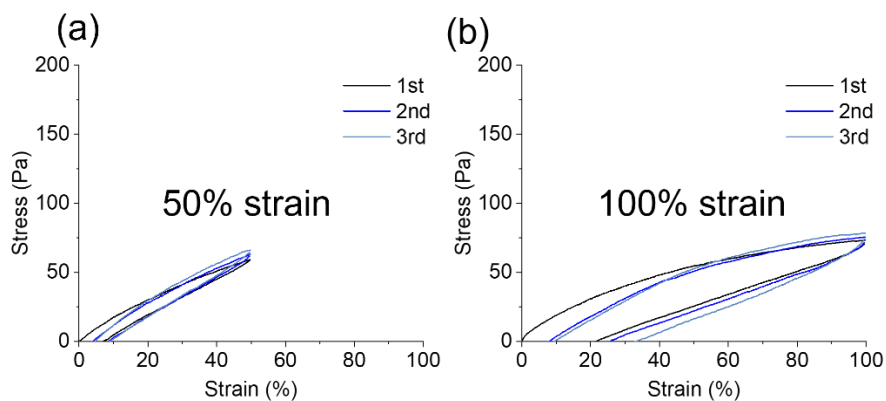


Figure S22. Cyclic loading and unloading of uniaxial stress tests of **PSR_{5wt}** with a strain rate of 20 $\mu\text{m/s}$ until (a) 50% and (b) 100% strain at 20 $^{\circ}\text{C}$.

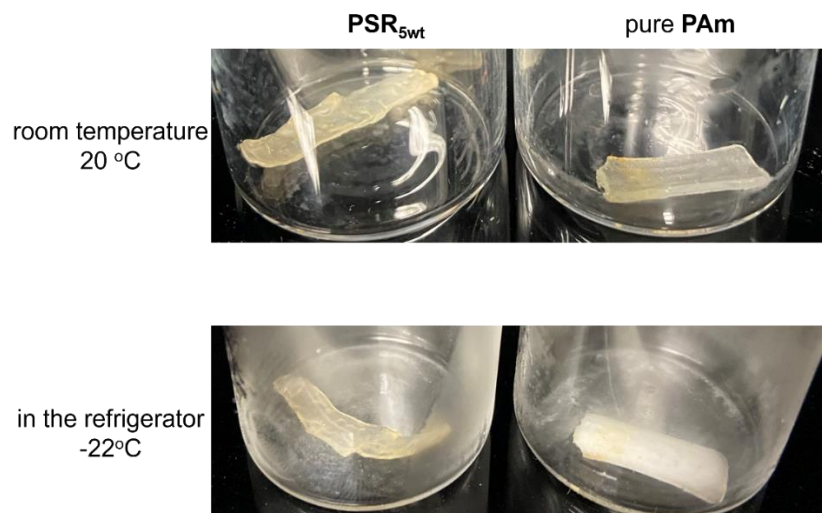


Figure S23. Image of **PSR_{5wt}** (left) and pure **PAAm** (right) at 20°C and -22°C.

Resistance change measurement at -14°C and 20 °C. The resistance change was measured by a combination of set-ups including a rheometer and a universal meter. The applied strains were controlled by the rheometer and the resistances at different strains were measured by the universal meter.

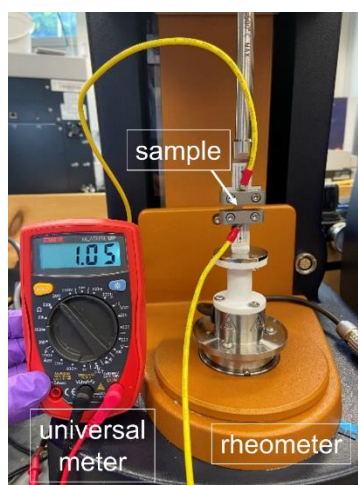


Figure S24. Image of the set-up used for the measurement of resistance of hydrogels under stretch.

Electrical conductivity measurements. The electrical conductivities at different temperatures were calculated by the resistance and dimensions of the hydrogels measured at different temperatures.

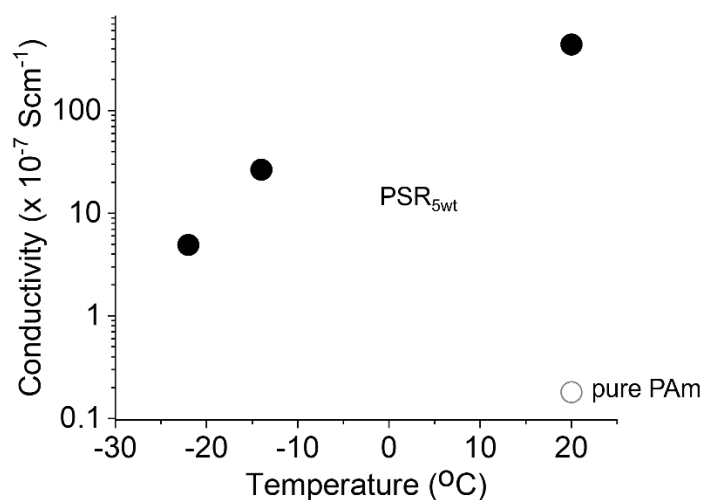


Figure S25. Electrical conductivity of **PSR_{5wt}** (solid circle) and **pure PAAm** (empty circle) hydrogels at different temperatures. The electrical conductivity of pure **PAAm** hydrogel is very close to that of pure water.

Fabrication of the finger motion sensor. The **PSR_{5wt}** hydrogel layer was molded in a shape of standard cuboid ($40 \times 8 \times 2$ mm) and then dried in a sealed chamber till the water content was lowered to 50 ± 3 %. The finger motion sensor was fabricated by molded **PSR_{5wt}** and cooper wires that were fixed onto a finger by tape. The cooper wire was linked to a universal meter to read the resistance change when the finger was bend or unbent. The measurements were conducted at room temperature (20 °C) and -14 °C (in a refrigerator). Before the measurement at low temperature, the strain sensor was pre-cooled in the refrigerator at -14 °C for 1 h.

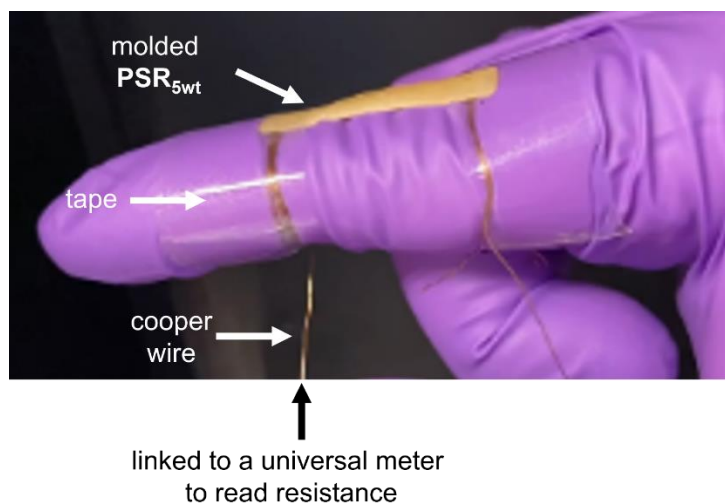


Figure S26. Image of the fabricated finger motion sensor by **PSR_{5wt}**, cooper wires and tapes.

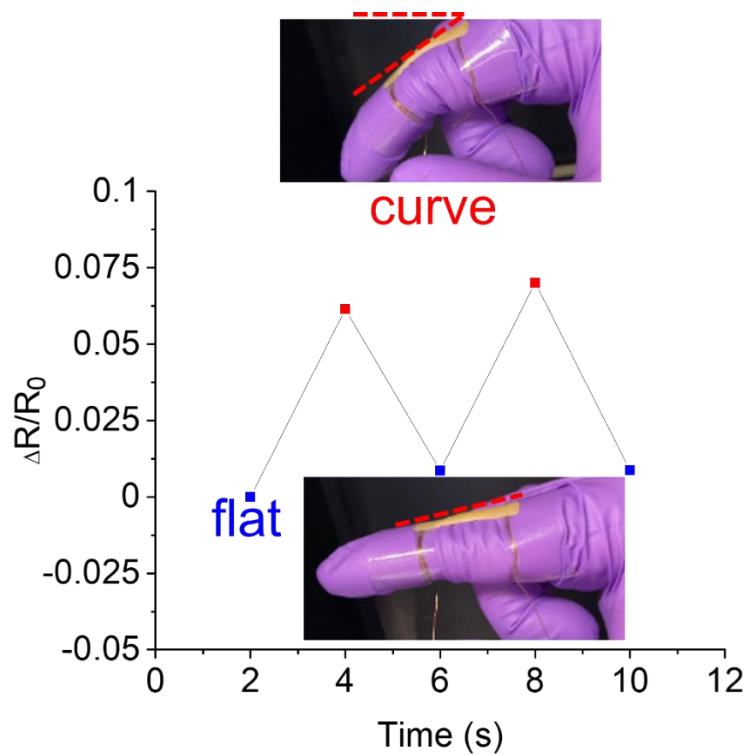


Figure S27. Resistance change of a PSR_{5wt} strain sensor as the finger bent and unbent at 20 °C.

Scanning electron microscope (SEM) experiments were conducted using a Thermo Scientific™ Helios™ 5 CX DualBeam. The samples for SEM analyses were prepared by lyophilizing the hydrogels frozen in liquid nitrogen.

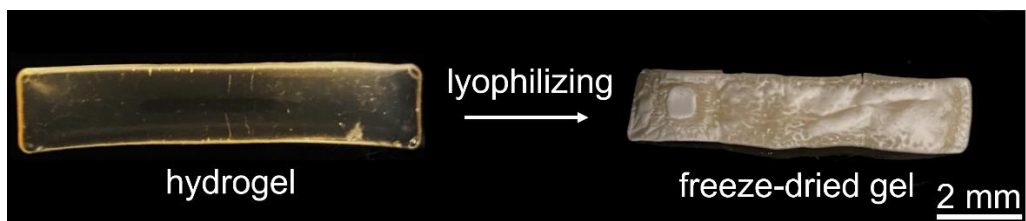


Figure S28. Images of PSR_{5wt} hydrogel before and after lyophilization.

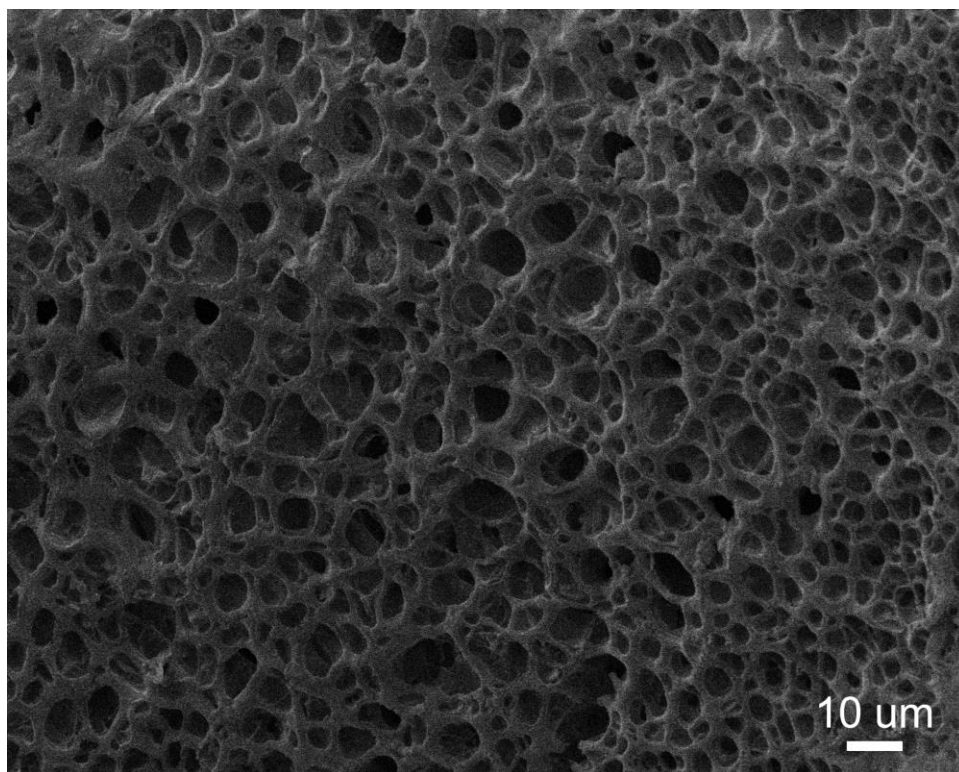


Figure S29. SEM image of PSR_{5wt} sample after lyophilization.

Table S2. Summary of the freezing point, strain at breakage (%) at 20 °C, and stress at breakage 20 °C of the reported anti-freezing hydrogels without adding salts and organic solvents.

literature	freezing point (°C)	strain at breakage (%) at 20°C	stress at breakage (KPa) at 20°C
This work	-25	750	175
<i>Matter</i> 2020 , 6, 820-822.	-30	/	/
<i>Mater. Horiz.</i> 2020 , 7, 919-927.	-26	1100	30
<i>Energy Environ. Sci.</i> 2019 , 12, 706–715.	-22	1050	100
<i>Adv. Funct. Mater.</i> 2018 , 28, 1704195	-20	220	75
<i>Chem. Eng. J.</i> 2019 , 372, 216-225.	-20	75	40
<i>J. Mater. Chem. A</i> 2020 , 8, 13787–13794.	-14	1550	210
<i>ACS Appl. Mater. Interfaces</i> 2021 https://doi.org/10.1021/acsami.1c08421	-7 & -10	200	20

References

1. J. Araki and K. Ito, *J. Polym. Sci. A Polym. Chem.* 2006, **44**, 6312-6323.